

# An Origami-Inspired Reconfigurable Suction Gripper for Picking Objects With Variable Shape and Size

Zhenishbek Zhakypov , Florian Heremans , Aude Billard , and Jamie Paik 

**Abstract**—Gripper adaptability to handle objects of different shape and size brings high flexibility to manipulation. Gripping flat, round, or narrow objects poses challenges to even the most sophisticated robotic grippers. Among various gripper technologies, the vacuum suction grippers provide design simplicity, yet versatility at low cost; however, their application is limited to their fixed shape and size. Here, we present an origami-inspired reconfigurable suction gripper to address adaptability with robotic suction grippers. Constructed from rigid and soft components and driven by compact shape memory alloy actuators, the gripper can effectively self-fold into three shape modes to pick large and small flat, narrow cylindrical, triangular and spherical objects. The 10-g few centimeters gripper lifts loads up to 5 N, 50 times its weight. We also present an underactuated prototype, demonstrating the versatility of our design and actuation methods.

**Index Terms**—Grippers, grasping, reconfigurable robots, foldable mechanisms, shape memory alloy.

## I. INTRODUCTION

**G**RIPPING is key to object manipulation and assembly. Besides delicacy and accuracy, adaptability of gripper geometry to the contact surface, and its mechanical compliance are important assets that bring high flexibility and dexterity for handling objects of different shape and stiffness, respectively. Numerous gripper technologies have been developed, from the most dexterous multi-finger robotic hands [1], two-finger grippers [2], conformable soft hands [3], [4], adhesion-based soft grippers [5] and universal jamming grippers [6], [7] to industrial vacuum suction grippers [8]. Though employing multi-degrees-of-freedom robotic fingers requires meticulous control of configuration and contact forces [9], [10], jamming grippers have limitations in handling flat or soft objects, and adhesion-based gecko grippers necessitate sophisticated clean-room microfiber

fabrication using lithography. Conventional soft vacuum suction grippers in the form of cups or bellows, on the other hand, overcome some of these challenges having simple, robust and low cost designs, but lack universality. There are a variety of fixed suction cup geometries from a few millimeters to a few decimeters circular-opening diameter, oval aperture for picking long objects, and with different compliance for lifting solid metal, fragile glass, or flexible textile fabric [11]. Hence, gripping objects of different shape and stiffness with a single cup is impossible without replacement, which is demanding and time consuming. Therefore, a self-reconfigurable suction gripper adaptable to any gripping task would increase flexibility and process efficiency.

Made from soft and deformable rubber material, a typical industrial suction cup ensures conformity and sealing to the contact interface [12]. However, if we would like to pick objects of different surface areas and stiffness, both the suction gripper geometry, i.e. the cross-sectional area of the mouth, should conform to object contour, as well as the compliance of the gripper. For example, picking a rigid aluminum profile is different to picking a relatively softer hamburger bun in that the latter requires a more delicate grip. This is challenging given the highly deformable nature of elastomers, which creates issues for accurate shape reconfiguration and control [13]. One prominent solution to the problem of reconfiguration and compliance lies in suction gripper morphology; multiple shapes of cross-sectional areas could effectively conform to object geometry and also create various stiffnesses associated with structural density [14]. Such metastructural and metamaterial behavior is the nature of robotic origami design [15], [16], where rigid facets connected with flexible hinges generate desired 3-D shape configurations [17]–[19] by self-folding, and different stiffness modes by collapsing the structure [20], locking some of the hinges [21], or by means of variable stiffness material joints [10], theoretically with infinite degrees of freedom (DoF) [22].

Here, we present a novel reconfigurable robotic origami suction gripper that combines versatility of origami folding design with conformity of soft elastomer material to address shape adaptability for suction grippers, as depicted in Fig. 1. Powered by shape memory alloy (SMA) actuators and vacuum, our proposed system effectively switches between three operating modes, producing large, small, and narrow openings to pick-and-place objects with flat, narrow cylindrical, triangular, and spherical surfaces. We demonstrate the load bearing capacity of the single suction gripper of more than 5 N, which is 50 times the gripper's weight, and ability to pick long objects as narrow

Manuscript received February 24, 2018; accepted June 5, 2018. Date of publication June 14, 2018; date of current version June 25, 2018. This letter was recommended for publication by Associate Editor Z. Xiong and Editor H. Ding upon evaluation of the reviewers comments. This work was supported in part by the SNSF “START” Project, in part by the Swiss National Center of Competence in Research (NCCR) Robotics, and in part by and the Sustainable Design of 4D Printed Active Systems (SD4D) funds. (*Corresponding author: Jamie Paik.*)

Z. Zhakypov and J. Paik are with the Reconfigurable Robotics Laboratory, Swiss Federal Institute of Technology Lausanne, Lausanne 1015, Switzerland (e-mail: zhenishbek.zhakypov@epfl.ch; jamie.paik@epfl.ch).

F. Heremans is with the Vrije Universiteit Brussels, Halle 1500, Belgium (e-mail: florian.roeland.heremans@vub.be).

A. Billard is with the Learning Algorithms and Systems Laboratory, Swiss Federal Institute of Technology Lausanne, Lausanne 1015, Switzerland (e-mail: aude.billard@epfl.ch).

Digital Object Identifier 10.1109/LRA.2018.2847403

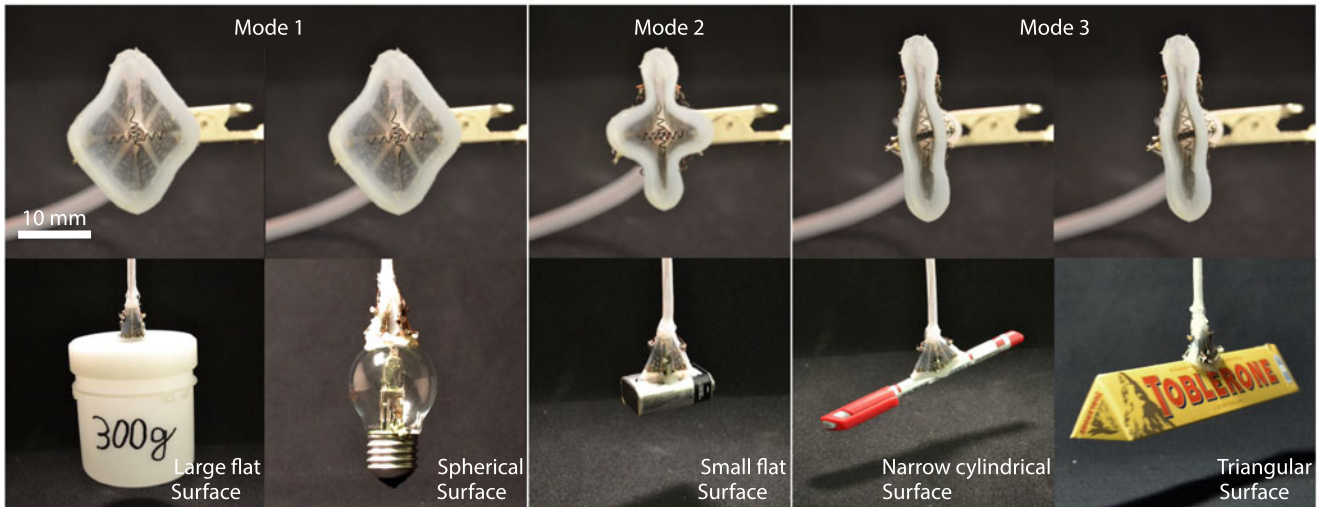


Fig. 1. The reconfigurable universal suction gripper in different modes. The gripper adapts to the object geometry and size, be it a large, small, or narrow planar object, or a cylindrical, or spherical object. In Mode 1, the gripper has the maximum opening area and can pick a container with a relatively large planar surface and a light bulb with spherical surface. In Mode 2, the gripper has a small opening and can grip a 9 V battery, impossible with Mode 1. In Mode 3, the gripper can pick an office pen of 10 mm diameter, as well as a triangular object, like the Swiss chocolate Toblerone.

as an office pen. We also propose a cable-driven under-actuated approach for the suction gripper to increase power efficiency. The main contributions of our work are

- Design and fabrication of a reconfigurable robotic origami suction gripper with three shape modes for pick-and-place of planar, cylindrical, triangular, and spherical objects.
- Demonstration of two compact actuation methods for gripper reconfiguration; SMA-based distributed actuation and cable driven under-actuation.
- Experimental validation of the gripper prototype with objects with various geometries and weight.

## II. SUCTION GRIPPER DESIGN

Gripping objects of different shape and size, requires reconfigurability of the suction gripper morphology to adapt to object form and maintain sealing by suction. Namely, the gripper's opening perpendicular to the object surface must be adjusted to conform to the object's profile; flat or non-flat. A universal system requires active switching between multiple opening modes, posing challenges to geometry, mechanisms and actuation design described next.

### A. Problem Formulation

Our goal is to design a suction cup with arbitrary cross-sectional area. In theory, a suction cup with an extremely small, flat circular-opening would conform to any arbitrary surface as it can be approximated by infinite planar surfaces. However, it would not be capable of lifting relatively heavy objects as the gripper's holding force is directly proportional to the opening surface area, given a perfect gripper-object sealing, expressed by

$$F = PA \quad (1)$$

where  $F$  is the holding force,  $P$  is the vacuum pressure inside the gripper and  $A$  is the gripper opening surface area. So, to

pick a cylindrical object, the cup opening should be non-flat to maximize the contact area on the 3-D surface, hence the holding force. Therefore, a universal suction gripper for picking flat, as well as round objects should not only have a planar opening, but also a non-flat conformable opening when necessary. Designing such a soft, deformable and simultaneously controllable cup structure is challenging due to unconfined DoF of soft materials. Soft elastic materials can bend, twist, compress, or stretch, which makes their modeling and control difficult.

To confine DoF and achieve accurate shape reconfiguration, the suction cup geometry should comprise rigid and compliant parts, similar to origami. Fig. 2(a) displays the approximation of a deep geometry conic shape suction cup with triangular rigid facets connected by revolute hinges. The number of right triangles  $n$  defines the accuracy of representing the conic shape, as well as DoF for achieving different flat opening geometries or modes  $m$ , when some of the hinges are folded in mountain or valley fashion. For instance, if  $n = 8$  the structure is a pyramid with a square opening, which also generates two other smaller flat opening modes, like a triangle or rhombus, upon folding of specific hinges, and infinitely many other non-flat opening surfaces. If  $n$  keeps increasing then the shape converges to cone and the number of flat modes increases accordingly. Each mode has a different area of opening and can be summarized by

$$A(n, m) = \frac{1}{4} \left( \frac{n}{2} - (m - 1) \right) r^2 \cot \left( \frac{\pi}{\frac{n}{2} - (m - 1)} \right) \quad (2)$$

where  $n$  and  $m$  are the number of right triangles and modes, respectively,  $r$  is the base length of the isosceles triangle formed by two right triangles.

The physical implementation and actuation of high numbers of hinges for shape reconfiguration poses difficulties as their number necessitates equal numbers of actuators. Therefore, practically, there is a limitation to the maximum achievable

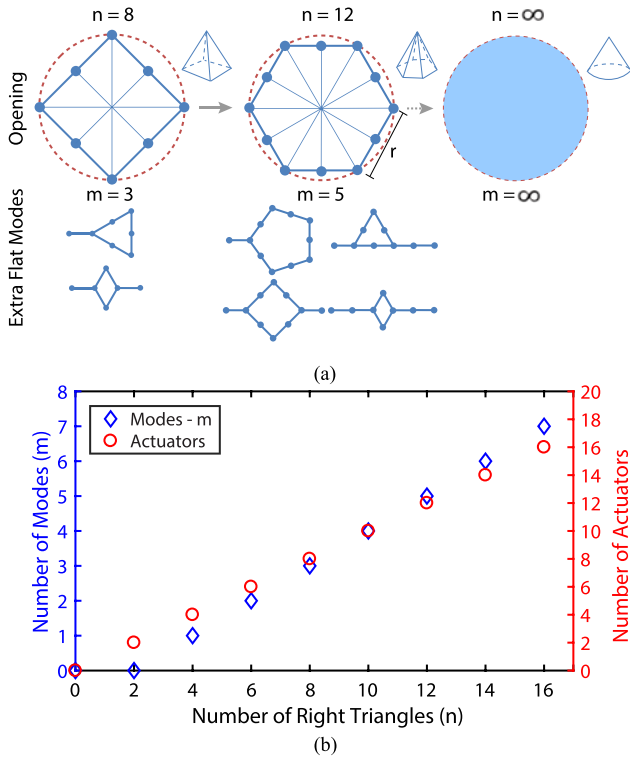


Fig. 2. The geometric approximation of a conic shape suction cup by rigid triangles connected with compliant hinges and producing number of cross-sectional opening modes by folding. (a) Connecting eight or higher number of right triangles in chain approximates the conic shape of the cup. Multiple modes of flat opening can be produced if some tiles are folded in valley or mountain fashion. Increasing the number of triangles  $n$  produces more flat opening modes  $m$ , hence more accurate representation of the conic suction cup. (b) The number of tiles versus the number of actuators and achievable number of modes plot. The number of tiles requires equal number of actuators, whereas the number of flat opening modes is proportional to the tile number.

modes and to maximize it, more compact actuation methods, as well as convenient fabrication process should be considered.

We propose a method to generate suction gripper multiple shape transformations by robotic origami and design the gripper using the robotic origami (Robogami) design methodology, we presented in [16]. The method enables construction of structurally soft robots and mechanisms from discrete functional material layers for structural backing, flexible hinges, actuation etc, fabricated rapidly in 2-D and assembled by folding into 3-D. Our design method for achieving a high number of shape modes is well-applicable, not only to suction gripper designs, but also to many other origami-based reconfigurable designs, like manipulators or robotic fingers. Hence, the method enables combination of the suction gripper with these designs to extend gripping capabilities with distributed actuation or under-actuation strategies.

### B. Geometry Design

For design simplicity, we constructed a vacuum suction gripper with eight rigid triangular tiles ( $n = 8$ ) connected in closed chain by flexure hinges, forming a quadrilateral pyramid as in Fig. 3. The structure has three flat opening modes (see Fig. 2) and a non-flat opening mode. The flat opening modes can pick

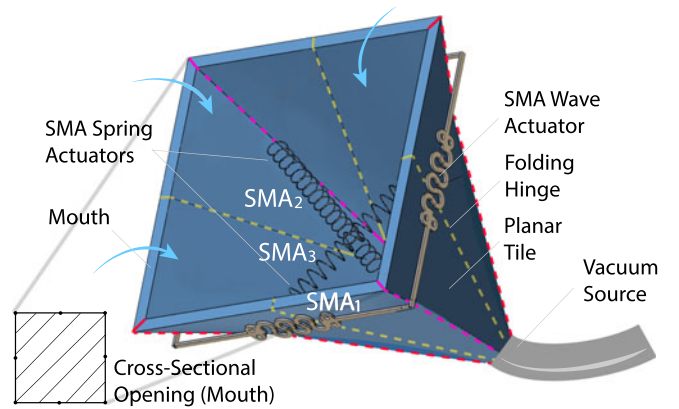


Fig. 3. The proposed origami suction gripper design. The pyramid-shaped suction gripper is constructed from eight triangular tiles connected with compliant hinges that fold in mountain (magenta and red lines) or valley (yellow lines) manner. A set of linear SMA actuators placed outside and inside the gripper enables self-folding to three shape modes.

large or small objects with planar or spherical surface, whereas the non-flat mode can handle narrow cylindrical or triangular objects. By connecting a vacuum source to the small nozzle section, the air flows into the large opening or mouth, creating suction when in contact with an object. To confine actuation, we chose only symmetric opening modes like a large square, small rhombic, or narrow rhombic opening shown in Fig. 4, described next.

*Mode 1:* In this mode, the suction gripper has a pyramid shape with a square opening at the base to allow picking relatively large and flat objects, whose size are at least the size of the opening. This mode has the maximum obtainable surface area (100%), hence the holding force for a given pressure is maximum.

*Mode 2:* In this mode, the opening shrinks due to folding of four valley hinges (yellow) inward, creating a small rhombic flat opening. When the two sets of tiles connected with the mountain hinge opposite to each other fold back-to-back, the other set produces angular spacing and the opening has a planar surface area. This is possible due to a slight difference between the triangular tile bases  $a$  and  $b$ . This mode enables precise gripping of small flat objects with 83% smaller size than for Mode 1.

*Mode 3:* In this mode, a long narrow non-flat rhombic opening is formed by folding the two diagonal mountain hinges (magenta) as in Fig. 4. This mode has two triangular protrusions out of plane. These protrusions, however do not prevent sucking cylindrical objects with diameter smaller than the gap  $g$ .

The geometry and arrangement of the triangular tiles play critical roles in achieving accurate shape transformation and define the surface area of the opening, which are governed by the following relations

$$A = \begin{cases} (a+b)^2 & \alpha = \frac{\pi}{2} & \text{Mode 1} \\ a^2 \sin \alpha & \alpha = \cos^{-1} \frac{b}{a} \ \& \ b < a & \text{Mode 2} \\ (a+b)^2 \sin \alpha & 0 < \alpha < \frac{\pi}{2} & \text{Mode 3} \end{cases}$$

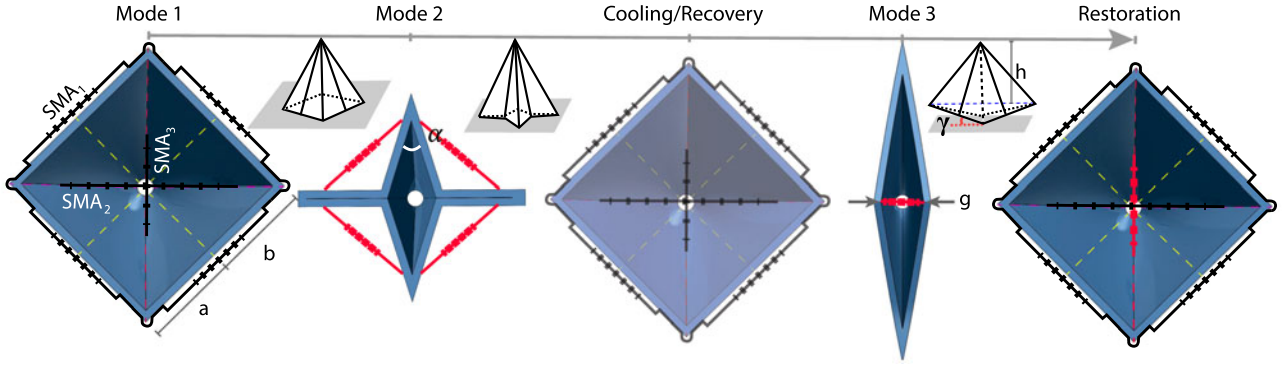


Fig. 4. The geometric design and actuator placement of the origami suction gripper. In Mode 1, the gripper is at rest and has a pyramid shape with eight planar tiles ( $n = 8$ ) connected with compliant mountain (magenta and red) and valley (yellow) hinges. By folding the hinges appropriately, two other gripper openings can be generated: Mode 2 and Mode 3. Six linear actuators are designed to compress (red) and enable folding for shape reconfiguration; four for valley folds and two for mountain folds.

For Mode 1 and Mode 2, the base length of the triangular tiles  $a$  and  $b$  and angular separation  $\alpha$  are fixed to ensure a flat contact with planar objects as in Fig. 4, whereas Mode 3 has many non-flat opening surfaces that can be expressed by  $\gamma$ , the angular elevation from contact plane, as follows

$$\sin \gamma = \frac{(a + b) \cos \alpha}{2 \cos \frac{\alpha}{2} \sqrt{h^2 + \frac{a^2}{4} - (a + b)^2 \sin^2 \frac{\alpha}{2}}} \quad (3)$$

Here,  $h$  is the distance between the blue dashed line connecting two farthest vertices and the one connecting all eight triangles and  $g$  is the gap between the two triangular protrusions. The gap can vary depending on the diameter of the cylindrical object.

### C. Folding Mechanisms Design

Three modes require selective folding of the joints in mountain or valley fashion. Utilizing conventional revolute hinges on the joints requires two kinematic pairs resulting in bulky and unsealed structure. Thus, to overcome this we designed elastic flexure hinges that fold upon bending moment, recover when at rest and ensure sealing. The bending motion can be induced by a bending actuator [23] placed in the same plane as the hinge or a compressing linear actuator across the hinge. The latter allows generating high moments with low linear strain [16], therefore favorable in our design.

The placement of linear actuators on the structure is critical to achieve shape reconstruction. A set of linear actuators  $SMA_1$ , when placed around the gripper in Mode 1, can compress to fold the four valley hinges inward, as shown in Fig. 4, producing Mode 2. The gripper shape can be partially recovered by the hinge elasticity when the actuators are disabled. One linear actuator  $SMA_2$  placed diagonally inside the gripper can contract and close the gripper diagonals to Mode 3. This actuator configuration minimizes loading effect on the outer set  $SMA_1$ . To ensure full recovery of the gripper from Mode 3 to Mode 1 in short time, another antagonistic pair  $SMA_3$  can be introduced perpendicularly below  $SMA_2$ , as in Fig. 4.

TABLE I  
ACTIVATION SEQUENCE AND TIME OF THE SMA ACTUATORS  
FOR GRIPPER RECONFIGURATION

Configuration	$SMA_1$	$SMA_2$	$SMA_3$	Delay (s)
Mode 1	Off	Off	Off	0
Mode 1→Mode 2	On	Off	Off	5
Mode 2→Mode 3	Off	On	Off	25
Mode 3→Mode 1	Off	Off	On	20
Mode 1→Mode 3	Off	On	Off	5

### D. Functional Materials Design

The folding mechanism of the suction gripper requires compression or extension of actuators when necessary. Employing linear DC motors at each hinge would make it bulky and rather expensive. Therefore, we opted for a functional material-based solution, particularly SMA actuators because of their compactness, high force-to-weight ratio, and customizable design. We designed a wave-type actuator and two spring-type actuators to enable hinge folding. All actuators compress when their temperature exceeds the phase transition temperature ( $M \rightarrow A$ ), upon Joule heating with direct current. Made of a thin Nitinol ( $Ni_{50\%}Ti_{50\%}$ ) sheet, the low-profile wave SMA actuator facilitates mounting on the suction gripper wall with negligible friction. It is also highly customizable in terms of force and stroke due to simplicity of arranging wave geometry (amplitude, frequency and line dimensions) and cycle by direct machining without forming, unlike spring SMA actuators. The activation sequence and time of the actuators and mode transitions are summarized in Table I.

Besides having high elasticity to restore shape at high angular deflection ( $\approx 180^\circ$ ), the hinge material should possess sealing properties to avoid air leakage. Silicone rubber is well-suited for this purpose, which comes with fabrication simplicity by molding. Among the several types of commercially available silicone elastomers, we selected the most suitable DragonSkin<sup>®</sup> 10 (Smooth-On Inc.) for high elasticity (475 psi), resistance to tearing (102 pli) and operational temperature ( $-53^\circ\text{C}$  to

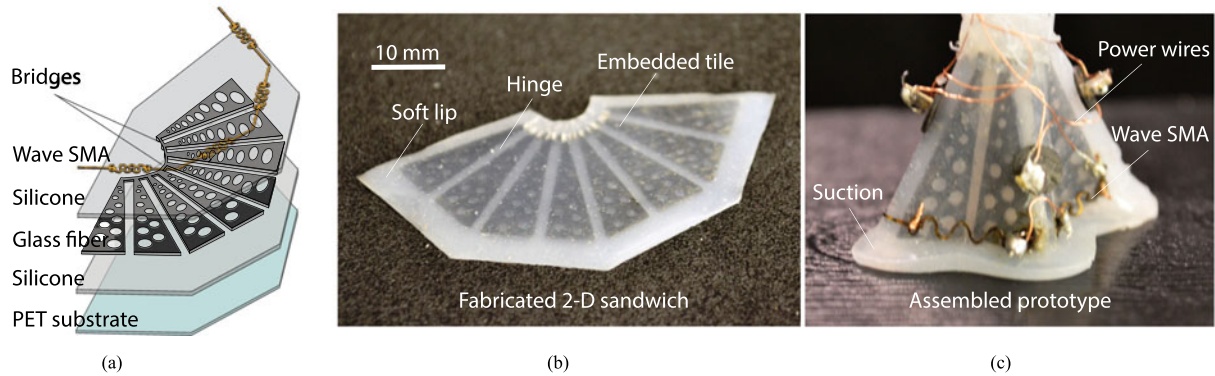


Fig. 5. (a) The rapid 2-D layer-by-layer fabrication process of the suction gripper and the fabricated prototypes in 2-D and 3-D. (b) The rigid fiberglass tiles are embedded between two silicone rubber layers to enable flexure hinges, conformity and sealing at the gripper opening. The wave SMA actuators are mounted lastly onto the sandwich. (c) The fabricated 2-D prototype without wave SMA actuator layer, which was folded and assembled to 3-D.

+232 °C). There is a myriad of possible materials for rigid tiles and we chose fiberglass due its high strength and low weight.

### III. FABRICATION

We fabricated our prototype employing 2-D processing method of discrete material layers, piling to multi-layer sandwich and assembly to 3-D, described next.

#### A. Suction Gripper Fabrication

The suction gripper construction necessitates both rigid backing and compliance for controlling shapes and conformity to the object. We embedded the triangular tiles into a silicone rubber (DragonSkin®) in a multi-layer process, as depicted in Fig. 5(a), and the sandwich in Fig. 5(b) is folded into a pyramid given in Fig. 5(c). The gripper is constructed from three layers; the outer two silicone layers embed the fiberglass tile layer. The silicone layers here not only serve as the flexure hinges, but also provide soft contact and sealing with the surface by means of lips. The lips protrude 5 mm from the rigid part, ensuring both foldability, compliance and sealing at the gripper opening.

To obtain the first layer, the liquid elastomer was poured onto a profiled PET sheet (positive mold) and spin-coated to 0.5 mm thickness and cured for 10 minutes in the oven at 90 °C. The tiles are cut from 0.4 mm thick fiberglass sheet employing a laser micromachining station (LAB 3550, Inno6 Inc.) with bridge spacers to ensure equal hinge spacing of 1.6 mm between the triangular tiles. The fiberglass layer is then placed onto the elastomer layer and another layer of liquid elastomer is poured onto the fiberglass. The sandwich is spin-coated and cured in the oven for one hour at 90° C. The holes on the fiberglass layer enable bonding of top and bottom elastomer layers by holding the tiles in place and preventing delamination. Finally, the PET support is removed, the wave SMA actuators are mounted and the bridge spacers on fiberglass cut out. The 1.5 mm thick sandwich is folded edge-to-edge to form a closed surface, and the two connecting ends are attached using silicone glue (Sil-Poxy™, Smooth-On Inc.). A 3 mm diameter flexible pipe

is attached to the small opening of the pyramid using silicone glue, which then connects to the vacuum source.

#### B. SMA Actuators Fabrication

SMA actuators require shaping and heat treatment process to induce the desired shape. In our design, all actuators were programmed to a compressed state. The set of four wave SMA actuators  $SMA_1$  with compressible wave-like pattern were cut out of a single 0.15 mm thick Nitinol sheet (Memry Corporation), as shown in Fig. 5(a). The 1 mm diameter holes at each section allows mounting the actuator onto the gripper's four walls (see Fig. 3) and the bridge connections are removed after mounting. To program the initial compressed shape, the series of actuators is annealed in a high temperature furnace (Nabertherm GmbH) at 400 °C for 30 minutes. After, the actuators are mounted on the suction gripper, fastened using wires and the connecting bridges are cut-out. Three wires connect the actuators in series and two power wires are finally attached to the actuator terminals to provide power.

Two spring SMA actuators are formed from a 0.25 mm diameter Nitinol wire (Dynalloy Inc.). The wire is wound around a 1 mm diameter steel rod with nearly 90° pitch angle and crimped at both ends. The rod is then placed into the furnace and annealed at 400 °C for 30 minutes.  $SMA_2$  actuator has seven coils, whereas the actuator  $SMA_3$  has five coils due to required shorter stroke. Both actuators are mounted perpendicularly to each other across the corner hinges diagonally (see Fig. 3), by pinching through the rubber from the inside and crimping at the outside. This configuration minimizes the loading effect on the actuator set  $SMA_1$ .  $SMA_2$  is mounted approximately 3 mm above  $SMA_3$ , therefore it requires a higher number of coils for longer stroke. Similarly, power wires are soldered on the crimps and the system is tested. After assembly, the gripper has opening dimensions of  $29 \times 29 \text{ mm}^2$  and height of 27 mm.

#### C. Hinge and Actuator Characterization

Force and deflection capabilities of SMA material and silicone hinges are highly influenced by their geometry, as well

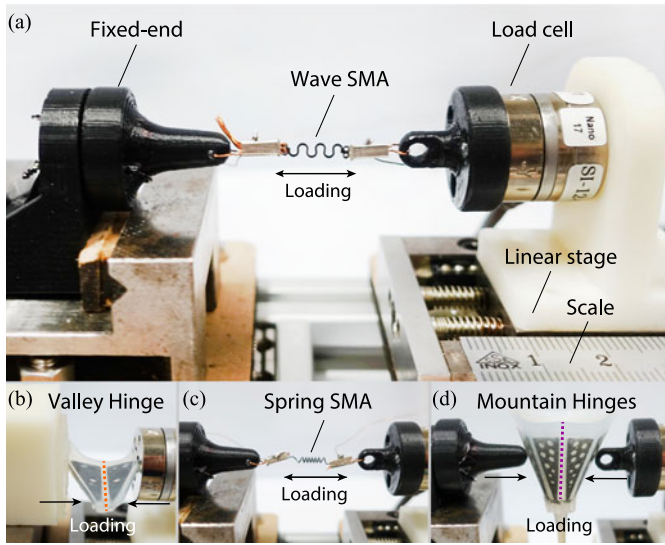


Fig. 6. The blocked force measurement setup for SMA actuators and rubber hinges. (a) The wave SMA actuator is clamped to the fixed part at one end and to the moving part with a load cell at the other end. The linear stage is moved to multiple positions and the actuator forces are measured for both austenite and martensite phases. (b) The valley hinge force characterization by bending. (c) The spring SMA mounted to the setup is tested similarly as the wave SMA. (d) The mountain hinge force measurement by compressing with two point tips from both sides.

as the fabrication process. Therefore, predicting their behavior without characterization is difficult or even impossible. To verify the capability of the SMA actuators in overcoming the hinge stiffness in austenite state (hot), we designed a loading setup depicted in Fig. 6(a). The setup consists of a fixed-end part and a moving part, which comprise a linear stage with mounted load cell (Nano 17, ATI Industrial Automation). The setup is employed to characterize the wave and spring SMA actuators blocked forces by extending them in both austenite and martensite phases, whereas the valley and mountain hinge stiffnesses are characterized by bending them under compression.

In the first test, we attached the wave SMA actuator ( $SMA_1$ ) with powering wires between the fixed and moving ends on the setup, as in Fig. 6(a). Initially, the actuator was in compressed state with length of 6 mm, then the stage is moved by 1 mm increments and the actuator force is measured by activating it at each position for 20 seconds to reach a steady-state force. The procedure is repeated three times per position and plotted with error bars in Fig. 7. The same test is performed for martensite case, from 6 mm to 9 mm elongation, with 1 mm deflection increment at room temperature. The produced force (see Fig. 7) was much lower than that of the austenite case as expected. The valley hinge (yellow) bending test is performed on the same setup by removing the tips on both ends and attaching a flat plate on the fixed-end as in Fig. 6(b). For this test, only a segment with two right triangle tiles connected with a rubber hinge is placed between the plate and the load cell surface. The hinge is pre-bent initially to overcome instability point and loaded by 1 mm increments and the forces at each position are recorded and plotted in Fig. 7. The hinge stiffness

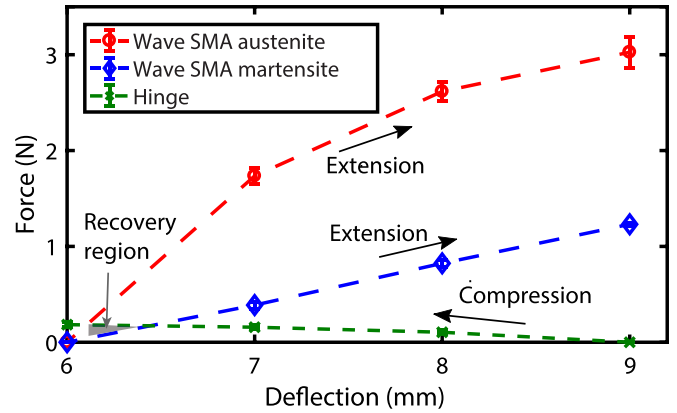


Fig. 7. The wave SMA actuator force plots in austenite and martensite states, and the valley hinge force response at different linear deflection. The triangular region reveals hinge folding when the actuator is in heating state (austenite) and the hinge partial recovery when the actuator is in cooling phase (martensite).

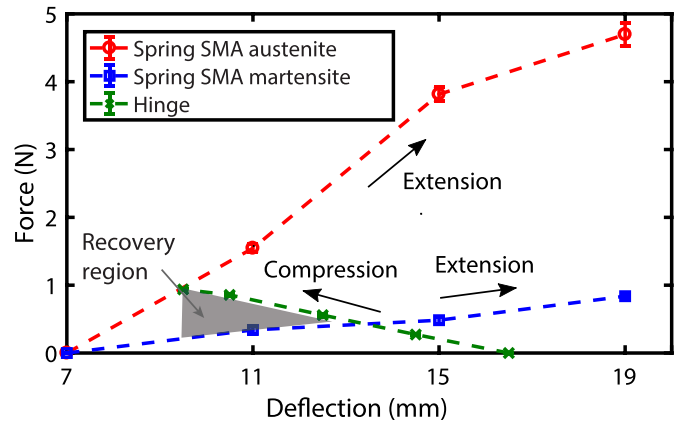


Fig. 8. The spring SMA actuator force response in austenite and martensite states, and the mountain hinge force at different deflections. The shaded triangular region shows the capability of the actuator to fold the hinge in heating phase (austenite) and the hinge's partial recovery when the actuator is in cooling process (martensite).

is lower than that of the actuator's in both austenite and martensite phases at high deflections, however it is higher at around 6 to 6.5 mm deflection at room temperature, highlighted by the shaded triangular region. This enables partial shape recovery of the suction gripper passively by extending the wave SMA actuators.

In the second test, the spring SMA actuator ( $SMA_2$ ) force is compared with the recovery forces of the mountain hinges (magenta). The loading procedure is the same as for the wave SMA for austenite and martensite phases [see Fig. 6(c)]. Due to higher stroke, the actuator was extended from 7 mm to 19 mm with 4 mm increments. Fig. 8 displays the austenite forces were considerably higher than the martensite forces. To measure the stiffness of the diagonal mountain hinges, the suction gripper is placed between the fixed-end and moving parts with point tips pressed to two diagonal edges, as in Fig. 6(d). The gripper is fixed at the bottom to ensure vertical alignment and loaded with increments of 2 mm from 16.5 mm opening distance to 9.5 mm. The hinge stiffness was lower than the spring SMA

at room temperature at high deflections, however, it was higher below 13 mm and could partially recover its shape in the cooling process of the actuator.

#### IV. EXPERIMENTAL RESULTS

To validate the reconfigurability of the suction gripper and its gripping performance, we conducted two experiments to study its shape reconfiguration to pick different objects and the holding force in all three modes.

The experimental setup is as follows: the suction gripper is connected to a  $-80$  kPa vacuum source and the actuators are connected to a controller board. The controller board comprises an Arduino microcontroller, three switches to regulate the power supply to three SMA actuators by PWM duty modulation and three push buttons to activate the actuators manually. PWM duty value of each actuator is calibrated to generate desired austenite finish temperatures of  $70$  °C for spring SMA and  $65$  °C for wave SMA, as specified in the vendors datasheets for wire and sheet Nitinol alloys, respectively.

##### A. Shape Reconfiguration

To test the effectiveness of the modes for gripping objects of different size, we selected five items to pick-and-place: a plastic container with large flat planar surface area, a 9 V DC battery with  $25 \times 44$  mm<sup>2</sup> planar surface area, an office pen with a diameter of 9.5 mm, Swiss chocolate Toblerone with triangular profile, and a spherical light bulb, as depicted in Fig. 1. The gripper is at rest in Mode 1 and could easily pick the large plastic container and the light bulb due to deep geometry. Then it was activated for 5 seconds to configure to Mode 2 to pick the battery that is too small to pick with Mode 1. Finally, the gripper was cooled for 20 seconds and activated for 5 seconds to configure to Mode 3 and pick the pen and chocolate, both successfully performed.

In this test, the gripper achieved the desired shapes accurately; however, the shape of the gripper was not maintained after contact with an object. The gripper shrunk to compensate for vacuum pressure, therefore the opening area decreased resulting in lower forces. This phenomena was observed in all three modes and is due to structural softness of the gripper. Also, in Mode 2, a slight push of the gripper perpendicularly to the battery surface was needed to ensure suction. This discrepancy is related to imperfection in the opening surface.

##### B. Holding Force

To evaluate the maximum holding force in each mode, we loaded the suction gripper, as in Fig. 9(a). Fig. 9(b) displays the measured and calculated holding forces. As the suction gripper shrinks radially under vacuum, we measured the actual opening areas to calculate the expected forces. To study the gripper opening area, suction is applied onto a flat transparent plastic for modes 1 and 2, whereas for Mode 3, a  $180^\circ$  bent transparent plastic with curvature of 9.5 mm is used. The vacuum pressure generated by the gripper was identical in all three modes at  $-80$  kPa and was measured using a digital pressure switch

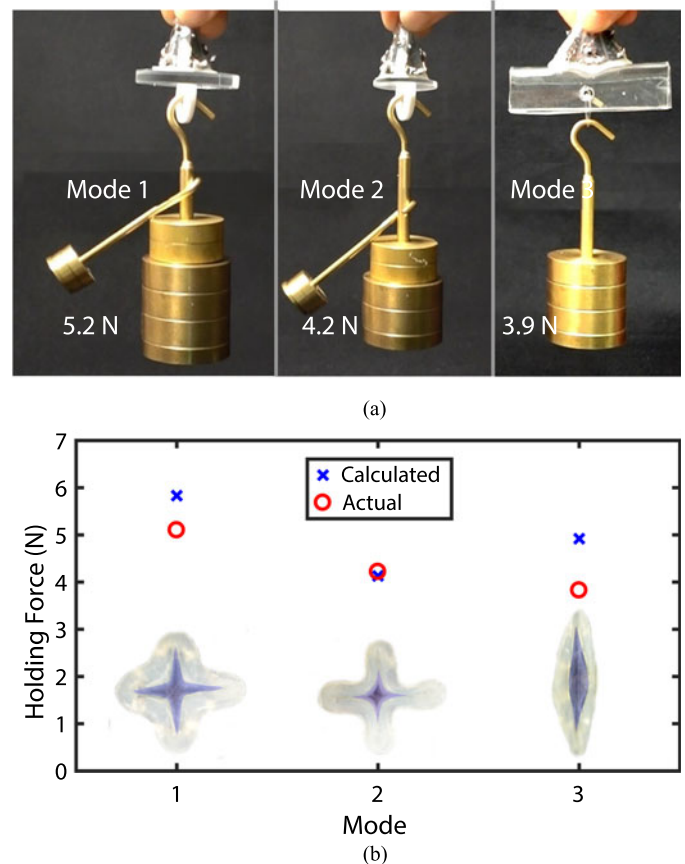


Fig. 9. The origami suction gripper holding force measurement test and plots. (a) For Mode 1, the gripper is attached to a flat round plate ( $d = 43$  mm) with a hole to hook weights. The gripper can lift up to 5.2 N weight. Similarly, a smaller plate ( $d = 29$  mm) is used for lifting weights up to 4.2 N with Mode 2. Finally, a bent acrylic plate with 9.5 mm curvature is employed for hooking weights up to 3.9 N in Mode 3. (b) The comparison between the actual and calculated holding forces in each mode. The expected forces are calculated by measuring the actual gripper opening area, shaded with blue, on a transparent surface at  $-80$  kPa vacuum pressure. The actual value is slightly lower than the analytic one for Mode 1 and comparably lower for Mode 3 due to imperfect sealing.

(ISE30A-01-P, SMC Corporation). The areas of the openings are then measured using image processing software (Image J) and used to calculate the holding forces by expression in (1).

The actual forces are measured by loading the suction gripper with weights in three modes, as in Fig. 9(a). Suction is first applied to a round flat plate of 43 mm radius for Mode 1, 29 mm radius for Mode 2 and a bent plate for Mode 3, with hooks for attaching weights. As expected, Mode 1 could hold the maximum load of 5.2 N (530 g), which is more than 50 times its weight, whereas Mode 2 could hold up to 4.2 N and Mode 3 up to 3.9 N. The loads are attached vertically and centered with minimal tangential effect and the weights are increased until the gripper eventually detaches from the plates. The maximum holding forces are plotted in Fig. 9(b), the error in predicting the expected forces was small for Mode 1 and 2 and comparably large in Mode 3 due to imperfect sealing between the curved surface and the suction gripper.

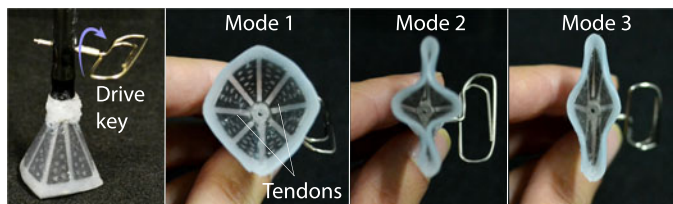


Fig. 10. An under-actuated approach for the reconfigurable suction gripper. A set of tendons (fishing wires) pass across the hinges and tiles and wound around the rotational drive key. The gripper is initially in Mode 1, then by rotation of the key switches to Mode 3. Further rotation will produce Mode 2.

## V. CONCLUSION AND DISCUSSION

In this letter, we present a reconfigurable suction gripper inspired by origami. With its multiple shape transformation modes, the robotic gripper can pick flat, cylindrical, triangular, and spherical surface objects. Three shape configuration modes enable changing the suction gripper's opening to effectively adapt to the object geometry and size. The embedded linear SMA actuators allow for a compact design and efficiently switch modes by selective activation. We demonstrate the efficacy of the gripper to pick objects with large and small planar surfaces, as well as more challenging object geometries like a narrow cylindrical office pen, a triangular object and a spherical light bulb. We evaluated holding forces for each mode and show the capability of the gripper for lifting loads up to 5 N, or 50 times its weight.

The distributed actuation method could be improved by a tendon driven under-actuated approach, as shown in Fig. 10. This approach necessitates minimum actuators to achieve multiple DoF, allowing low-weight construction and design scalability. Here, a rotational pin pulls or releases tendons (fishing wires) inside the gripper. The shape transformation between Mode 1 and 3 occurs upon rotation of the key in one direction and further rotation produces Mode 2. The key could be replaced by a DC motor with encoder for closed loop control of the shape reconfiguration, solving the issue of accuracy and efficiency.

The current prototype still faces limitations in suction forces and sealing due to shrinkage under vacuum pressure. We plan to include an extra layer of variable stiffness material, such as shape memory polymer, to achieve shape reconfiguration in soft mode and maintain gripper shape while sucking in stiff mode. Our design approach is extendable to suction grippers with tunable compliance for handling soft or brittle objects. In this sense, different structural stiffness modes should be studied along with added functional material layers with adjustable stiffness properties.

## REFERENCES

[1] C. Gosselin, F. Pelletier, and T. Laliberte, "An anthropomorphic underactuated robotic hand with 15 DOFs and a single actuator," in *Proc. IEEE Int. Conf. Robot. Autom.*, 2008, pp. 749–754.

[2] B. Belzile and L. Birglen, "A compliant self-adaptive gripper with proprioceptive haptic feedback," *Autonomous Robots*, vol. 36, no. 1–2, pp. 79–91, 2014.

[3] R. Deimel and O. Brock, "A novel type of compliant and underactuated robotic hand for dexterous grasping," *Int. J. Robot. Res.*, vol. 35, no. 1–3, pp. 161–185, 2016.

[4] Y. She, C. Li, J. Cleary, and H. J. Su, "Design and fabrication of a soft robotic hand with embedded actuators and sensors," *J. Mechanisms Robot.*, vol. 7, no. 2, 2015, Art. no. 021007.

[5] S. Song, D. M. Drotlef, C. Majidi, and M. Sitti, "Controllable load sharing for soft adhesive interfaces on three-dimensional surfaces," *Proc. Nat. Academy Sci.*, pp. E4344–E4353, 2017.

[6] E. Brown *et al.*, "Universal robotic gripper based on the jamming of granular material," *Proc. National Academy Sci.*, vol. 107, no. 44, pp. 18809–18814, 2010.

[7] J. Kapadia and M. Yim, "Design and performance of nubbed fluidizing jamming grippers," in *Proc. IEEE Int. Conf. Robot. Autom.*, 2012, pp. 5301–5306.

[8] C. C. Kessens and J. P. Desai, "A self-sealing suction cup array for grasping," *J. Mechanisms Robot.*, vol. 3, no. 4, 2011, Art. no. 045001.

[9] M. G. Catalano, G. Grioli, E. Farnioli, A. Serio, C. Piazza, and A. Bicchi, "Adaptive synergies for the design and control of the Pisa/IIT SoftHand," *Int. J. Robot. Res.*, vol. 33, no. 5, pp. 768–782, 2014.

[10] A. Firouzeh and J. Paik, "Grasp mode and compliance control of an underactuated origami gripper using adjustable stiffness joints," *IEEE/ASME Trans. Mechatronics*, vol. 22, no. 5, pp. 2165–2173, Oct. 2017.

[11] K. Tai, A. R. El-Sayed, M. Shahriari, M. Biglarbegian, and S. Mahmud, "State of the art robotic grippers and applications," *Robotics*, vol. 5, no. 2, pp. 11–31, 2016.

[12] T. J. Elliott and A. J. Staines, "Sheet-gripping sucker," U.S. Patent US6557845B2, Harris-Intertype Corp, Melbourne, FL, USA, 1964.

[13] D. Rus, and M. T. Tolley, "Design, fabrication and control of soft robots," *Nature*, vol. 521, no. 7553, pp. 467–475, 2015.

[14] S. Li and K. W. Wang, "Fluidic origami: A plant-inspired adaptive structure with shape morphing and stiffness tuning," *Smart Materials Structures*, vol. 24, no. 10, 2015, Art. no. 105031.

[15] A. Firouzeh and J. Paik, "Robogami: A fully integrated low-profile robotic origami," *J. Mechanisms Robot.*, vol. 7, no. 2, 2015, Art. no. 021009.

[16] Z. Zhakypov and J. Paik, "Design methodology for constructing multimaterial origami robots and machines," *IEEE Trans. Robot.*, vol. 34, no. 1, pp. 151–165, Feb. 2018.

[17] E. B. Hawkes, N. M. An, H. Benbernou, S. Tanaka, E. D. Kim, D. R. Demaine, and R. J. Wood, "Programmable matter by folding," *Proc. Nat. Academy Sci. United States Amer.*, vol. 107, no. 28, pp. 12441–12445, 2010.

[18] S. Miyashita, S. Guitron, S. Li, and D. Rus, "Robotic metamorphosis by origami exoskeletons," *Sci. Robot.*, vol. 2, no. 10, 2017.

[19] Z. Zhakypov, M. Falahi, M. Shah, and J. Paik, "The design and control of the multi-modal locomotion origami robot, Tribot," in *Proc. IEEE/RSJ Int. Conf. Intell. Robot. Syst.*, Sep. 2015, pp. 4349–4355.

[20] S. M. Felton, D. Y. Lee, K. J. Cho, and R. J. Wood, "A passive, origami-inspired, continuously variable transmission," in *Proc. IEEE Int. Conf. Robot. Autom.*, 2014, pp. 2913–2918.

[21] J. Kim, D. Y. Lee, S. R. Kim, and K. J. Cho, "A self-deployable origami structure with locking mechanism induced by buckling effect," in *Proc. IEEE Int. Conf. Robot. Autom.*, 2015, pp. 3166–3171.

[22] C. Sung, E. D. Demaine, M. L. Demaine, and D. Rus, "Edge-compositions of 3D surfaces," *J. Mechanical Design*, vol. 135, no. 11, 2013, Art. no. 111001.

[23] Z. Zhakypov, J. L. Huang, and J. Paik, "A novel torsional shape memory alloy actuator: Modeling, characterization, and control," *IEEE Robot. Autom. Mag.*, vol. 23, no. 3, pp. 65–74, Sep. 2016.